Supplemental Figure 1

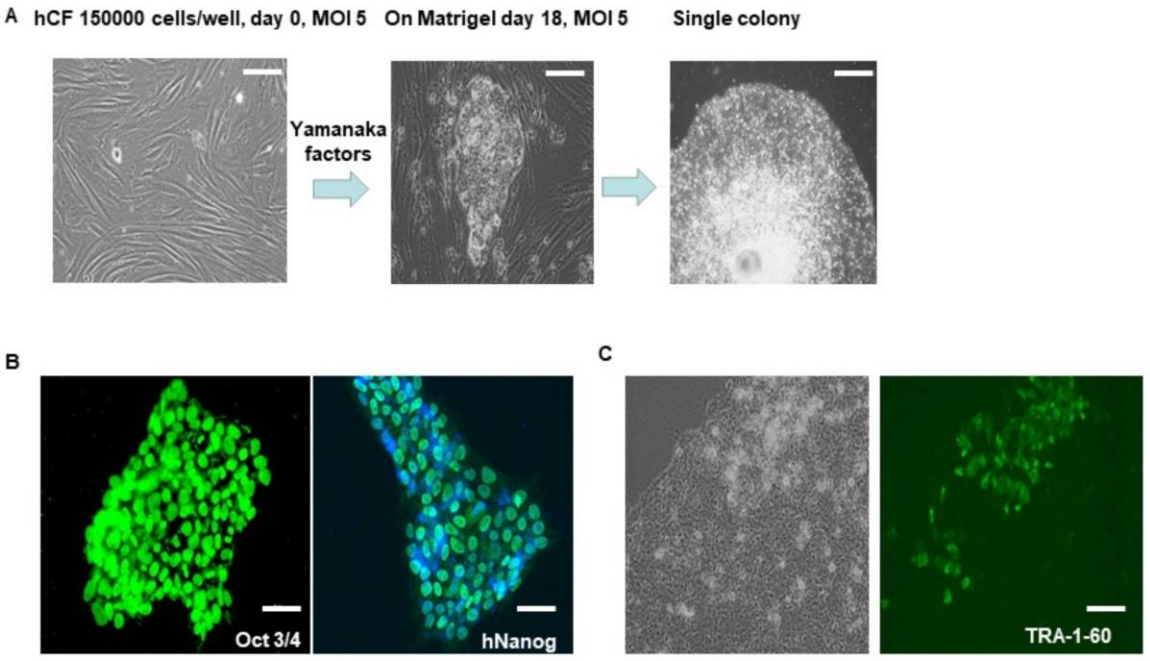

Supplemental Figure 1. Reprogramming of human cardiac fibroblasts (cFs). A and B- Microscopic imaging. A) Bright field imaging of cFs transduced with non-integrating Sendai virus expresing Klf4, Oct3/4, Sox2 and cMyc, scale bar 100 µm. **B)** Immunofluorescence of pluripotency markers Oct3/4 (left) and hNanog (right), scale bar = 50 µm **C)** Bright field (left), and immunofluorescence of TRA-1-60 (right), scale bar 100 µm. Multiplicity of infection (MOI) is 5.

Supplemental Figure 2

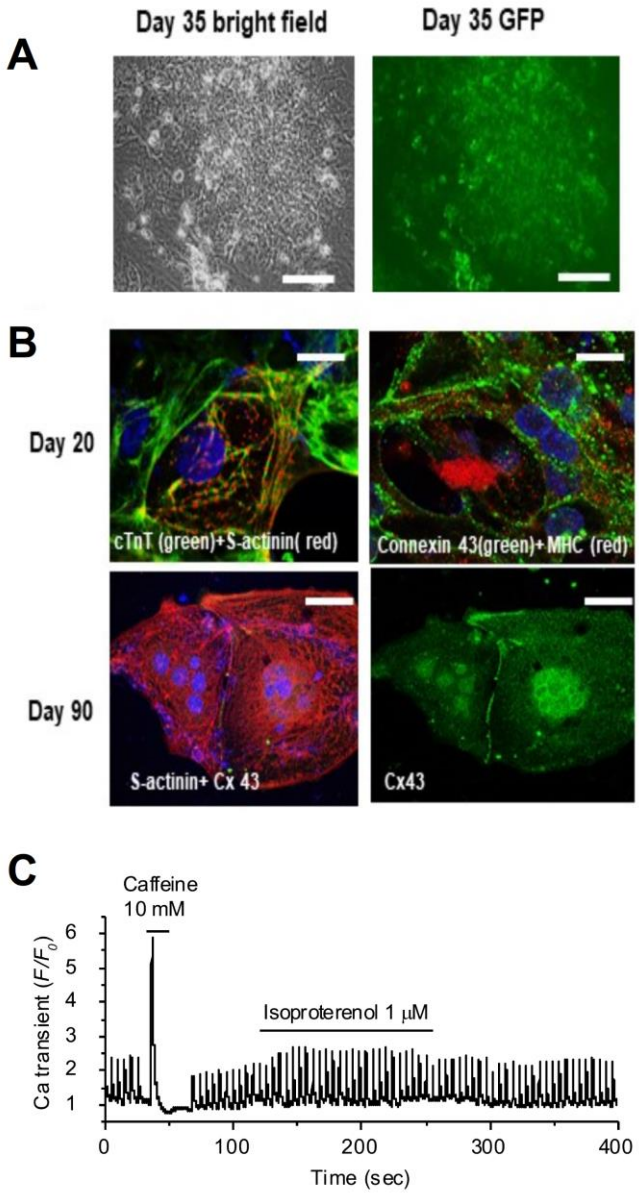

Supplemental Figure 2. Analysis of dermal fibroblast-derived hiPSC-CMs (dFCM). **A)** Differentiated dFCMs expressing αMHC-eGFP at day 30 of differentiation. Left: bright field. Right: GFP signal. Scale bar = 100 μm. **B)** Immunofluorescence staining of cardiac markers. Top right: cTnT2 and cardiac s-actinin at day 20 of differentiation. Top left: Cx43 and MHC at day 20 of differentiation. Bottom left: s-actinin+Cx43 at day 90 of differentiation. Bottom right: Cx 43. Scale bar = 100 μm. Scale bar = 10 μm. **C)** Calcium transient measurements at day 30 using fluo-4 as fluorescent dye. A representative trace depicting spontaneously beating and pacing in dFCMs. T_{50}=300 msec. Caffeine (10 mM) stimulation, followed by isoproterenol (1 μM) stimulation**.**

Supplemental Figure 3

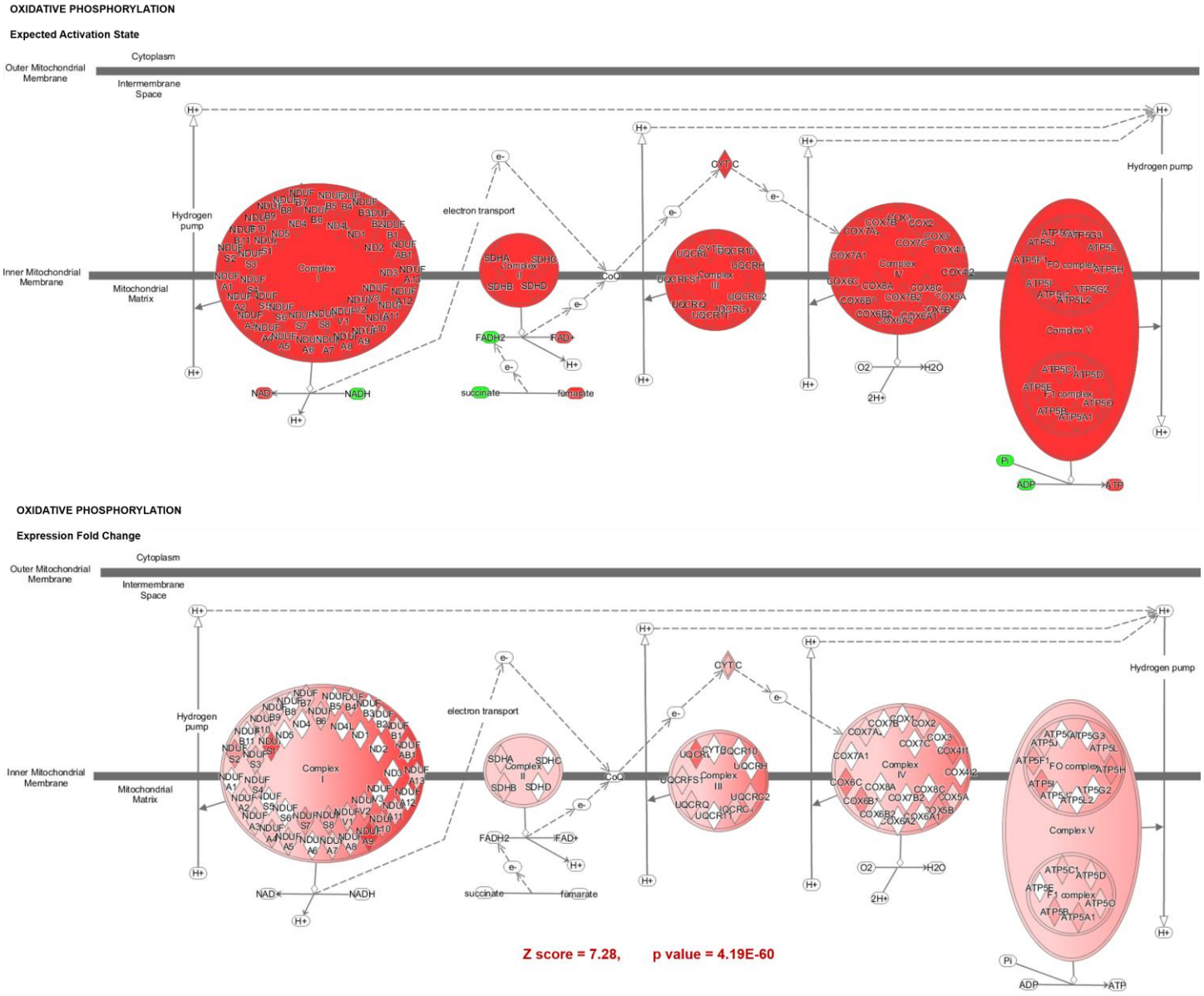

Supplemental Figure 3. Canonical OXPHOS pathway prediction by IPA. *Top*- Predicted direction of molecules in OXPHOS signaling pathway in cFCMs at day 115 versus day 12 as in the IPA knowledge base. *Bottom*- Observed fold change in expression with the z-score and p-value.

Supplemental Figure 4

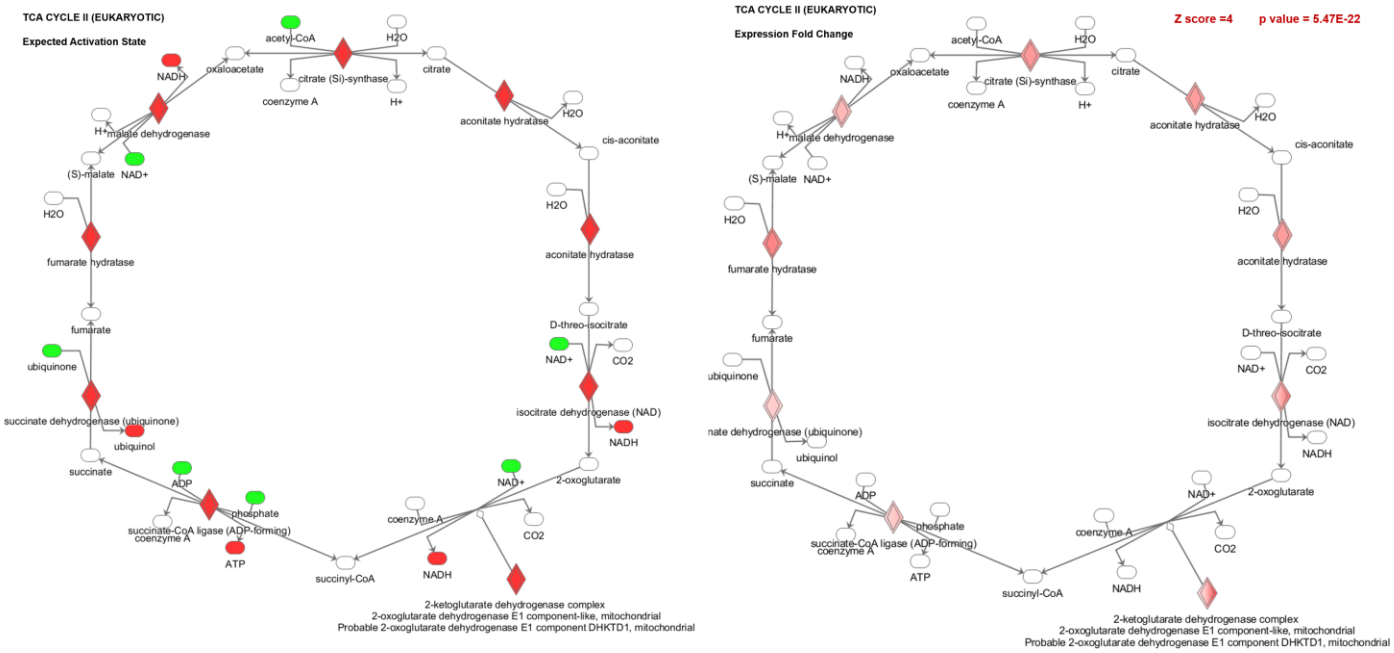

Supplemental Figure 4. Canonical TCA pathway prediction by IPA. *Left*- Predicted direction of molecules in TCA pathway in cFCMs at day 115 versus day 12 as in the IPA knowledge base. *Right*- Observed fold change in expression with the z-score and p-value.

Supplemental Figure 5

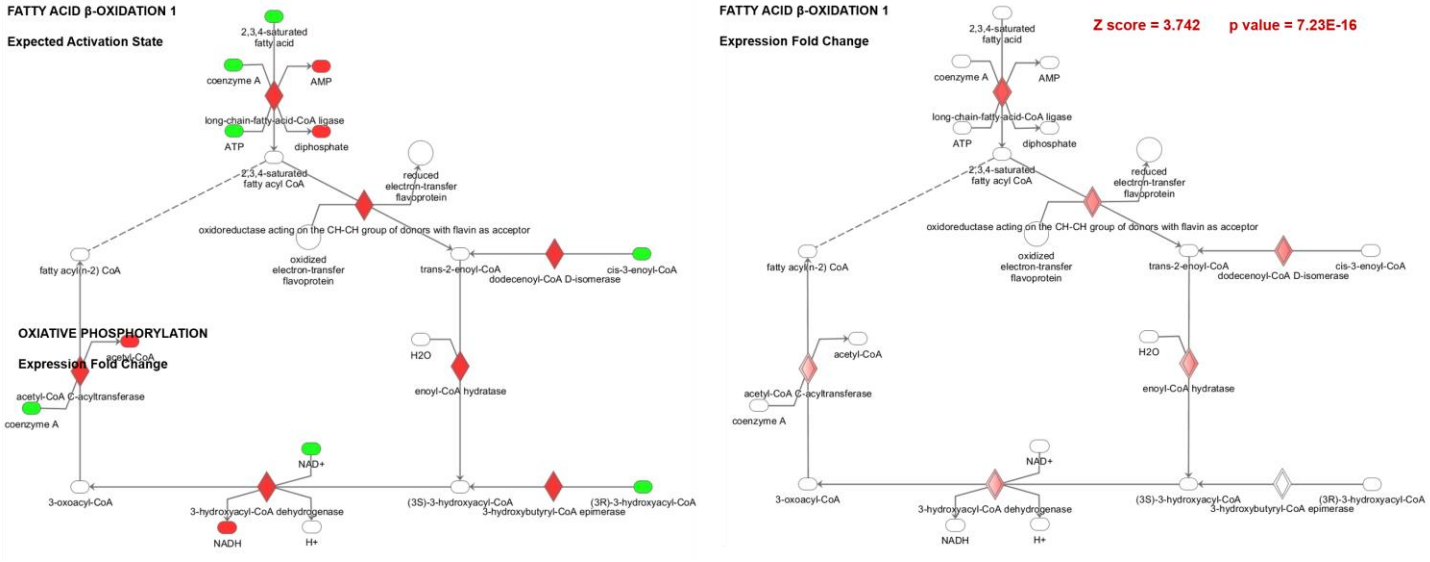

Supplemental Figure 5. Canonical FAO pathway prediction by IPA. *Left*- Predicted direction of molecules in FAO pathway in cFCMs at day 115 versus day 12 as in the IPA knowledge base. *Right*- Observed fold change in expression with the z-score and p-value.

Supplemental Figure 6

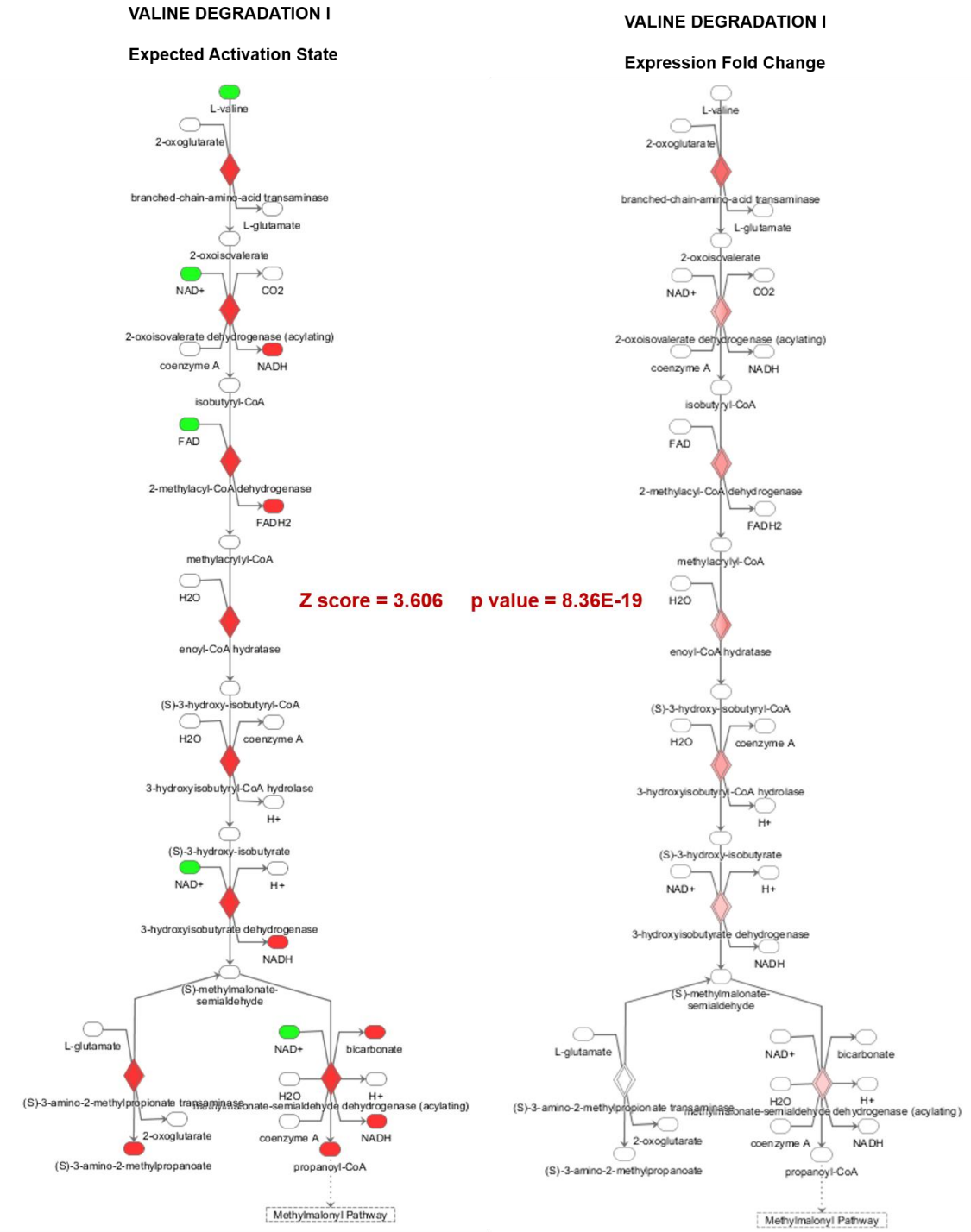

Supplemental Figure 6. Canonical valine degradation I pathway prediction by IPA. *Left*- Predicted direction of molecules in cFCMs at day 115 versus day 12 in valine degradation I pathway as in the IPA knowledge base. *Right*- Observed fold change in expression, with the z-score and p-value.

Supplemental Figure 7

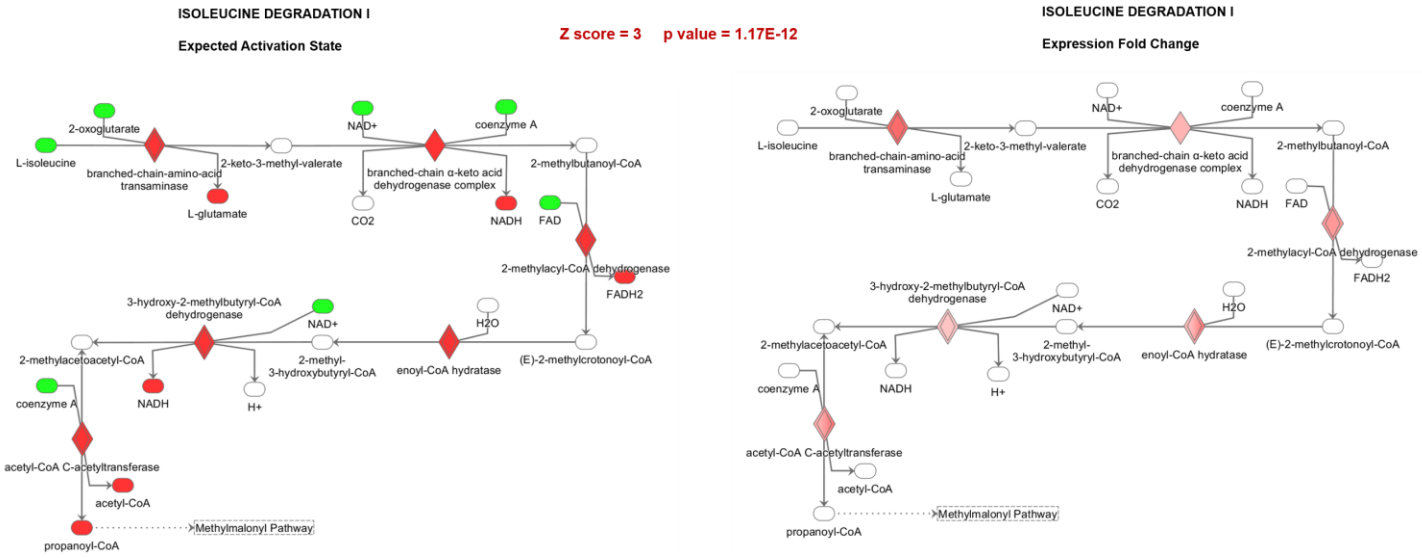

Supplemental Figure 7. Canonical isoleucine degradation I pathway prediction by IPA. *Left*- Predicted direction of molecules in cFCMs at day 115 versus day 12 in isoleucine degradation I pathway as in the IPA knowledge base. *Right*- Observed fold change in expression, with the z-score and p-value.

Supplemental Figure 8

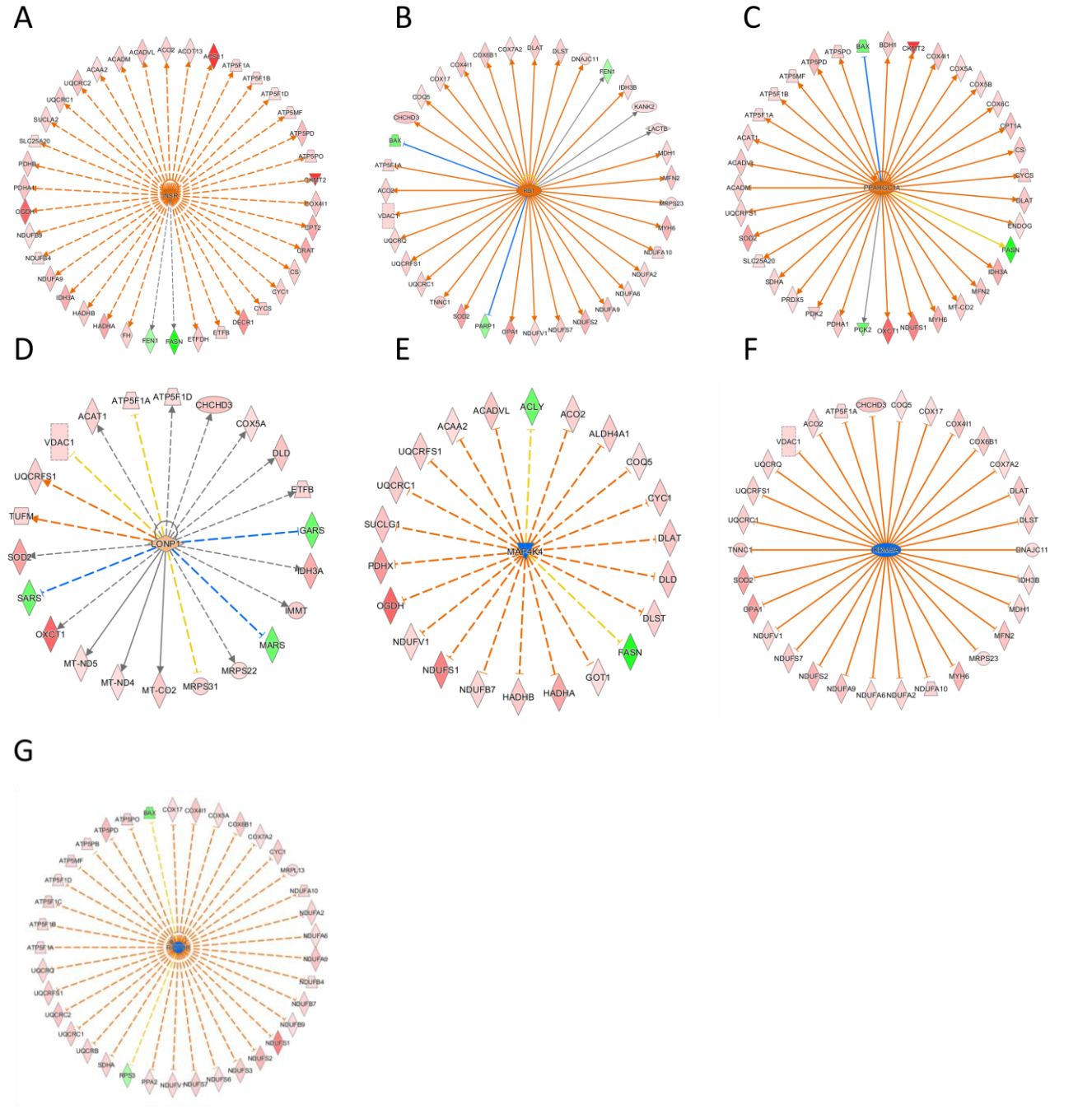

Supplemental Figure 8. Predicted upstream regulators identified in in cFCMs at day 115 versus day 12 by IPA**. A)** PPARGC1A regulator network. **B)** INSR regulator network. **C)** RICTOR regulator network. **D)** RB1 regulator network. **E)** KDM5A regulator network. **F)** **MAP4K4** regulator network. **G)** LONP1 regulator network.

Supplemental Figure 9

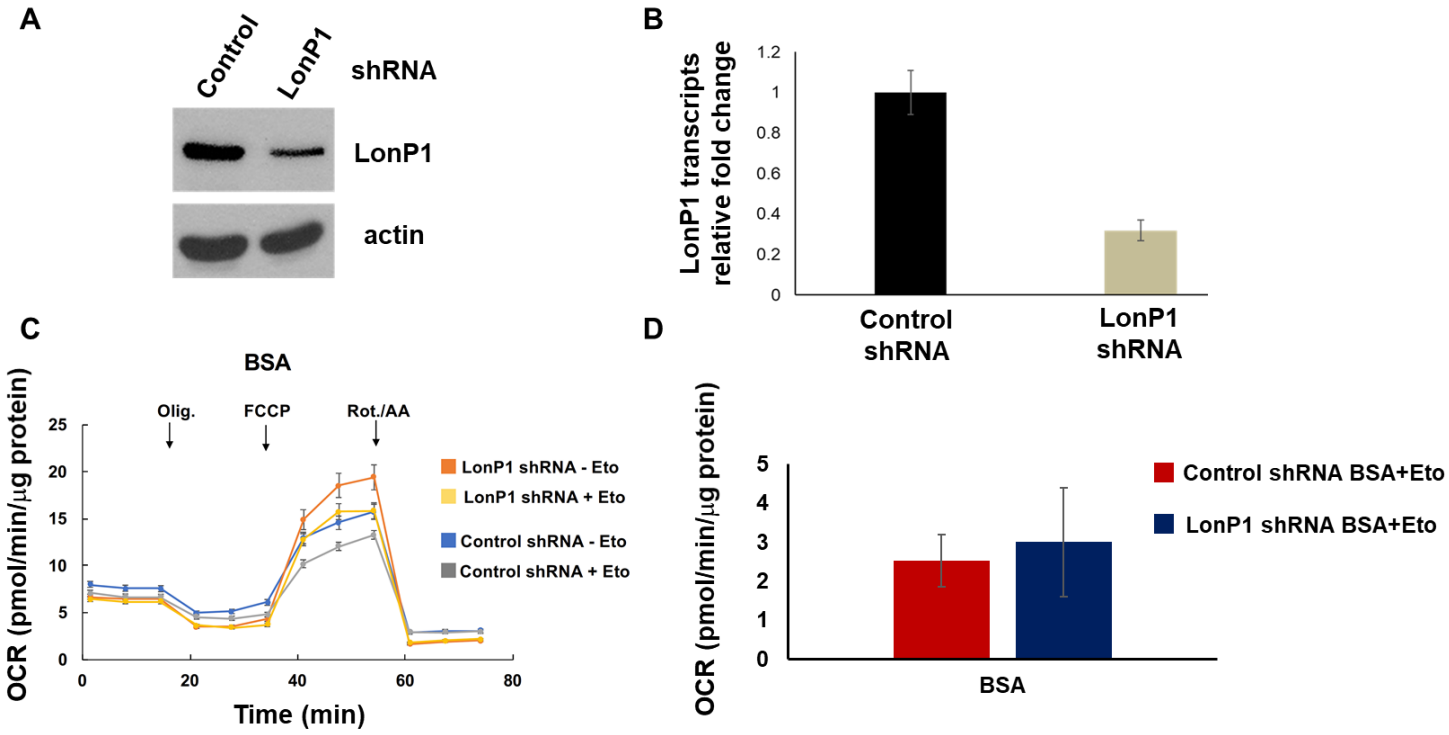

Supplemental Figure 9. Effect of LonP1 down regulation on fatty acid oxidation in nRVMs. A) Immunoblot showing the downregulation of LonP1 in nRVMs after transducing with control or LonP1 shRNA adenoviral particles for 4-5 days. Actin is used as a loading control. B) Relative fold change in LonP1 transcript levels in LonP1 shRNA nRVMs compare to control. 18S transcript was used as an endogenous control. C) Measurement of oxygen consumption rate (OCR) in isolated nRVMs, subjected to mito stress test after supplementing with BSA (100μM) as a control for Palmitate-BSA in the presence or absence of Etomoxir (40μM), an inhibitor of fatty acid oxidation. D) FAO was measured as a difference in OCR between none and etomoxir treated nRVMs (± BSA). Data values are mean ± SEM.